JOURNAL OF THERMOPHYSICS AND HEAT TRANSFER
Vol. 19, No. 4, October–December 2005

Modeling Radiative Properties of Silicon with Coatings and Comparison with Reflectance Measurements

B. J. Lee* and Z. M. Zhang†
Georgia Institute of Technology, Atlanta, Georgia 30332
and
E. A. Early,‡ D. P. DeWitt,§ and B. K. Tsai¶
National Institute of Standards and Technology, Gaithersburg, Maryland 20899

Achieving high-accuracy temperature measurements in rapid thermal processing using radiation thermometry requires knowledge of the optical properties of silicon and related materials, such as silicon dioxide, silicon nitride, and polysilicon. However, available optical property models lack consistency and are not fully validated by experiments at the wavelength and temperature ranges critical to radiation thermometry. A critical survey is given of the existing optical models, with emphasis on the need for extrapolation and validation. Also described is an algorithm for calculating the radiative properties of lightly doped silicon with coatings. The effect of coatings covering one or both sides of a smooth silicon wafer is theoretically studied at room temperature, as well as at elevated temperatures. A spectrophotometer was used to measure the reflectance for selected samples in the wavelength region from 0.5 to 1 μm at room temperature. The measurements agree well with the predicted reflectance for bare silicon, a silicon wafer with a nitride coating, and wafers with an oxide coating of different thicknesses, whereas a larger deviation of as much as twice the measurement uncertainty is observed for a silicon wafer coated with polysilicon and oxide films.

Nomenclature

d	=	thickness, μm
k	=	extinction coefficient
n	=	refractive index
T	=	temperature, °C
α	=	absorption coefficient, cm^{-1}
ε	=	emittance
θ	=	polar angle, deg
λ	=	wavelength in vacuum, μm
ρ	=	reflectance
σ_{st}	=	standard error of estimate
τ	=	transmittance
τ_i	=	internal transmittance

Subscripts

a	=	air
b	=	bottom
c	=	calculation
f	=	thin film
m	=	measurement
s	=	substrate
t	=	top

Introduction

THE continual development toward shrinking device sizes and increasing patterning density has made conventional batch furnaces inadequate for a number of processes. In the mean time, rapid thermal processing (RTP), which is a single-wafer integrated circuit fabrication process, has become a key technology for semiconductor device manufacturing in a variety of applications, such as thermal oxidation, annealing, and thin-film growth.[1,2] Temperature measurement and control have been a critical issue for continuous improvement and implementation of RTP to meet the requirements of technology development.[3] In RTP, the heating source is at a much higher temperature than that of the silicon wafer, and radiative energy exchange is a dominant mode of heat transfer. Therefore, understanding the radiative properties of silicon and other relevant materials is critical to analyze the thermal transport processes. Because many RTP furnaces use a noncontact radiometric temperature measurement scheme, accurate determination of the wafer emittance is necessary for correlating the radiance temperature to the true temperature of the wafer.[4]

Radiative properties such as reflectance, transmittance, and emittance depend on direction and wavelength, as well as wafer temperature. The radiative properties are also affected by thin-film coatings and surface roughness. The effect of surface roughness on radiative properties has been the subject of many studies.[5–8] For optically smooth surfaces, radiative properties can be theoretically calculated based on the thickness of each material in the multilayer structure and their optical constants.[9,10] Similarly, the optical constants generally depend on the wavelength of the incident radiation and the temperature of the silicon wafer.

There have been numerous studies on the optical and radiative properties of silicon materials. The fundamental physics of the crystalline structure, electron and phonon dispersion, and scattering mechanisms has been well established.[11] The absorption processes, associated with the band-gap absorption, free-carrier absorption, and lattice absorption, are well understood. Model expressions, which relate the optical constants or sometimes the dielectric function to wavelength and temperature, have been developed to cover certain spectral and temperature ranges with good accuracy. However, even though numerous functional expressions for the optical constants of silicon exist, none of them covers the entire range of wavelengths and temperatures of interest. The extrapolation of some of the expressions to the wavelength region between 0.8 and 1.0 μm, which is important for radiation thermometry, and to temperatures above 500°C is necessary. Furthermore, when expressions

Received 22 September 2004; revision received 13 December 2004; accepted for publication 14 December 2004.

*Graduate Research Assistant, George W. Woodruff School of Mechanical Engineering.
†Associate Professor, George W. Woodruff School of Mechanical Engineering. Associate Fellow AIAA.
‡Physicist, Optical Technology Division.
§Faculty Appointment, Optical Technology Division.
¶Physical Scientist, Optical Technology Division.

from different research groups are extrapolated to the same wavelength and temperature ranges, the differences in the calculated optical constants are significantly larger than the required uncertainties, especially at high temperatures, as will be shown in the next section.

Hebb[12] incorporated the functional expressions for the optical constants of silicon into an algorithm based on thin-film optics to calculate the radiative properties of silicon wafers with various doping levels. The software, known as Multi-RAD, has been used by others as a tool to predict the radiative properties.[13] Because different expressions for the refractive index of silicon were used, there appears to be a discontinuity, which becomes more prominent at elevated temperatures, in the calculated reflectance spectrum of lightly doped silicon at the wavelength $\lambda = 0.8$ μm. Furthermore, the adopted expression for the refractive index of silicon at wavelengths longer than 0.8 μm has not been fully validated. Timans[14] comprehensively reviewed the radiative properties of semiconductors and other relevant materials. Although the expressions from different sources were provided and the limitations addressed, he did not address the issue of discontinuity or uncertainty in the extrapolation of different model expressions beyond the wavelength or temperature range suggested in the original publications.

The ultimate goal of this project is to identify and, if needed, to develop reliable and experimentally validated optical property models that cover the spectral and temperature ranges of importance for RTP applications. The present paper provides a critical survey of the existing functional expressions for the optical constants of silicon. A computational algorithm is described for calculating the radiative properties of a dielectric substrate with thin-film coatings on one or both sides. A spectrophotometer is used to measure the specular reflectance of five samples in the wavelength region from 0.5 to 1.0 μm at room temperature. By a comparison of the measured and calculated reflectance, this work evaluates the reliability of the expressions for the refractive index of silicon and coating materials.

Survey of Optical Property Models

The optical constants, including the refractive index n and the extinction coefficient k of a material, are functions of wavelength and temperature. They also depend on the crystalline structure and doping and impurity levels. In the present work, emphasis is given to lightly doped (doping concentration $\leq 10^{15}$ cm^{-3}) single-crystal silicon because of its common use in the semiconductor industry.

Measurement data of the optical constants of silicon over wide wavelength regions at room temperature can be found in Ref. 15. However, fewer experimental data exist at high temperatures. Sato[16] was the first to study comprehensively the emittance of silicon wafers by a direct measurement, as well as by deducing it from the reflectance and transmittance measurements in the temperature range between room temperature and 800°C. However, the refractive index values based on his experimental data are consistently higher than those obtained from recent studies. In this section, several expressions of the optical constants of silicon are reviewed and compared to determine the most suitable model.

Refractive Index of Silicon

Jellison and Modine[17] measured the ratio of the Fresnel reflection coefficients of silicon wafers in both polarization states with a two-channel spectroscopic ellipsometer in the temperature range from 25 to 490°C. From the measurement results, they extracted the refractive index and extinction coefficient using the least-squares Levenberg–Marquardt fitting. The Jellison and Modine (J–M) expression of the refractive index for wavelengths between 0.4 and 0.84 μm is given as

$$n_{\text{J–M}}(\lambda, T) = n_0(\lambda) + \beta(\lambda)T \tag{1}$$

where

$$n_0 = \sqrt{4.565 + \frac{97.3}{3.648^2 - (1.24/\lambda)^2}}$$

$$\beta(\lambda) = -1.864 \times 10^{-4} + \frac{5.394 \times 10^{-3}}{3.648^2 - (1.24/\lambda)^2}$$

where λ, in micrometers, is the wavelength in vacuum and T, in degrees Celsius, is the temperature. These units will be used throughout this paper for all expressions.

Li[18] extensively reviewed the refractive index of silicon. By carefully analyzing published experimental data, he developed a functional relation, based on the modified Sellmeier-type dispersion relation, for the refractive index of silicon that covers the wavelength region between 1.2 and 14 μm and the temperature range up to 480°C. In Li's original expression, the temperature unit was Kelvin, and in the following equations, we have converted it to degrees Celsius:

$$n_L(\lambda, T) = \sqrt{\varepsilon_r(T) + g(T)\eta(T)/\lambda^2} \tag{2}$$

where

$$\varepsilon_r(T) = 11.631 + 1.0268 \times 10^{-3}T + 1.0384 \times 10^{-6}T^2 - 8.1347 \times 10^{-10}T^3$$

$$g(T) = 1.0204 + 4.8011 \times 10^{-4}T + 7.3835 \times 10^{-8}T^2$$

$$\eta(T) = \exp\left(1.786 \times 10^{-4} - 8.526 \times 10^{-6}T - 4.685 \times 10^{-9}T^2 + 1.363 \times 10^{-12}T^3\right)$$

Magunov[19] and Magunov and Mudrov[20] measured the temperature dependence of the refractive index at 1.15 and 3.39 μm and empirically approximated measurement results and built a relation that covers the wavelength region between 0.6 and 10 μm, in the temperature range from room temperature to 430°C. The Magunov and Mudrov (M–M) expression is

$$n_{\text{M–M}}(\lambda, T) = 3.413 + 1.782 \times 10^{-4}T + 4.365 \times 10^{-8}T^2 + \left(0.1635 + 2.400 \times 10^{-5}T + 1.389 \times 10^{-7}T^2\right)\lambda^{-2.33} \tag{3}$$

Figure 1a shows the refractive index of silicon at 25 and 800°C, for wavelengths from 0.5 to 1.5 μm. The refractive index decreases slightly as the wavelength increases. The squares indicate the refractive index data collected in Ref. 15. Notice that all of the expressions are extrapolated to 800°C. At room temperature, the refractive index values based on each expression agree well with the data in Ref. 15. Because no experimental data exist at wavelengths between 0.84 and 1.1 μm, the J–M and the Li expressions are separately extrapolated to this wavelength region, which is between the two vertical dash–dot lines. The refractive index obtained from these expressions differs when compared in the extrapolated region, and the difference becomes larger at higher temperatures. A difference in the refractive index may cause an error in the prediction of radiative properties and in the temperature measurement by radiation thermometers. For example, when extrapolated to 1000°C at a wavelength of 0.95 μm, the refractive index calculated from the J–M and M–M expressions are 3.877 and 4.012, respectively. The difference in the refractive index of 0.135 will result in an error of 2% in the calculated normal emittance of a bare silicon wafer. The effect on a radiation thermometer is a temperature error of more than 2°C. Note that many radiation thermometers commonly used for RTP applications operate at around 0.95 μm. Therefore, thorough study of the radiative properties in the wavelength region between 0.80 and 1 μm is important.

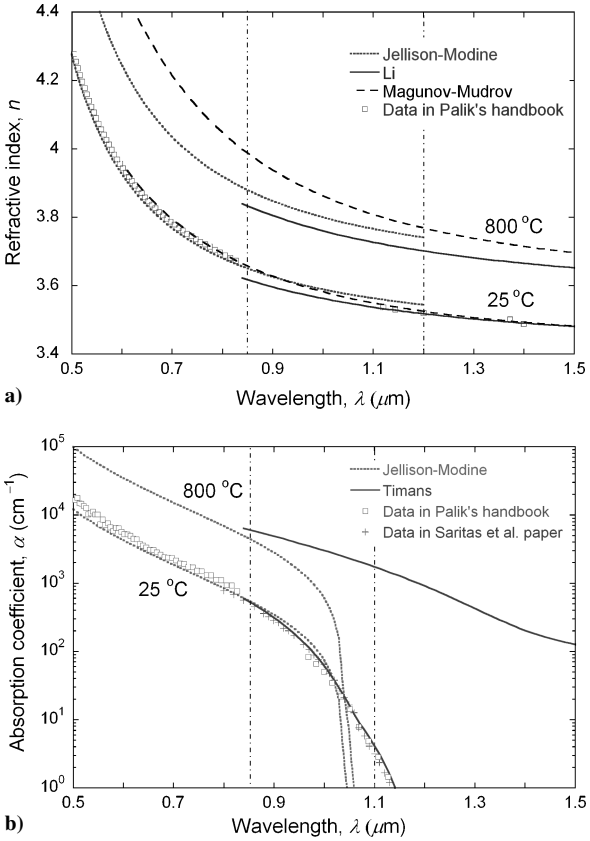

Fig. 1 Optical constants of silicon at selected temperatures: a) refractive index and b) absorption coefficient; two vertical dash–dot lines, extrapolation region of expressions for optical constants of silicon.

Extinction Coefficient of Silicon

The extinction coefficient k and absorption coefficient α are related by $\alpha = 4\pi k/\lambda$. The absorption coefficient of silicon depends on the absorption process such as interband transition, intraband transition, and free-carrier absorption. When the photon energy is higher than the band gap energy of silicon, electrons in the valance band can be excited to the conduction band, resulting in a large absorption coefficient. The J–M expression of the extinction coefficient, covering the wavelength range from 0.4 to 0.84 μm, is given as[17]

$$k_{\text{J–M}}(\lambda, T) = k_0(\lambda)\exp\{T/[369.9 - \exp(-12.92 + 6.831/\lambda)]\} \tag{4}$$

where

$$k_0(\lambda) = -0.0805 + \exp\left[-3.1893 + \frac{7.946}{3.648^2 - (1.24/\lambda)^2}\right]$$

The absorption coefficient can be deduced from the extinction coefficient.

Timans[21] measured the emission spectra of several silicon wafers in the longer wavelength region and deduced the absorption coefficient in the wavelength region from 1.1 to 1.6 μm, in the temperature range between 330 and 800°C. He suggested that the absorption coefficient can be expressed as a summation of the band-gap absorption and free-carrier absorption, as follows:

$$\alpha(\lambda, T) = \alpha_{\text{BG}}(\lambda, T) + \alpha_{\text{FC}}(\lambda, T) \tag{5}$$

The expression for the band-gap absorption can be found in the work by MacFalane et al.[22] and is given by

$$\alpha_{\text{BG}}(\lambda, T) = \sum_{i=1}^{4}\alpha_{a,i}(\lambda, T) + \sum_{i=1}^{2}\alpha_{e,i}(\lambda, T) \tag{6}$$

Notice that silicon is an indirect-gap semiconductor and that the absorption process is accompanied by either the absorption of a phonon, denoted by $\alpha_{a,i}(\lambda, T)$, or the emission of a phonon, denoted by $\alpha_{e,i}(\lambda, T)$. Detailed expressions for $\alpha_{a,i}(\lambda, T)$ and $\alpha_{e,i}(\lambda, T)$ can be found in Refs. 14 and 21. The band-gap absorption disappears at wavelengths longer than that corresponding to the energy gap (modified by the phonon energy).

For the free-carrier absorption, Sturm and Reaves[23] suggested an expression based on their measurement of the transmission of the wafer at 1.30 and 1.55 μm and in the temperature range of 500 to 800°C. The Sturm and Reaves (S–R) expression is

$$\alpha_{\text{FC}} = n_e A_e + n_h A_h \tag{7}$$

where n_e and n_h are electron and hole concentrations and A_e and A_h are electron and hole absorption cross sections, respectively. The S–R expression agrees well with experimental results in the wavelength region between 1.0 and 1.5 μm, but departs from experiments at longer wavelengths. Vandenabeele and Maex[24] studied the free-carrier absorption of silicon in the infrared region by measuring the emission from double-side-polished silicon wafers at wavelengths of 1.7 and 3.4 μm, in the temperature range from 400 to 700°C. They proposed a semi-empirical relation for calculating the extinction coefficient as a function of wavelength and temperature due to free-carrier absorption. The Vandenabeele and Maex (V–M) expression is

$$\alpha_{\text{FC}}(\lambda, T) = 4.15 \times 10^{-5}\lambda^{1.51}(T + 273.15)^{2.95}\exp\left(\frac{-7000}{T + 273.15}\right) \tag{8}$$

Here again, T is in degrees Celsius. Rogne et al.[25] demonstrated that the absorption coefficient calculated from the V–M expression agrees well with experimental data in the wavelength region between 1.0 and 9.0 μm at elevated temperatures.

The absorption coefficient of silicon at 25 and 800°C is shown in Fig. 1b. The squares represent the values converted from the extinction coefficient in Ref. 15 and the plus-marks indicate the data by Saritas and McKell.[26] Because no theoretical functions exist in the wavelength region between 0.84 and 1.1 μm, the J–M expression is extrapolated to longer wavelengths, whereas the expression by Timans coupled with the V–M free-carrier absorption formula is extrapolated to shorter wavelengths. When extrapolated, the absorption coefficient calculated from the J–M expression drops to zero at wavelengths longer than about 1 μm. Note that the J–M expression is extrapolated to elevated temperatures, whereas the Timans expression is extrapolated to room temperature because the original expression was developed at 300°C and above. The agreement between the calculated extinction coefficient values and the measured data from both Refs. 15 and 26 is very good at room temperature. However, as in the case of the refractive index, the disagreement between the expressions increases with temperature. Furthermore, no experimental data are available above 800°C for wavelengths shorter than 1.1 μm.

Other Materials

Because of a lack of experimental data, assumptions have to be made for the optical constants of silicon-related materials such as silicon dioxide, silicon nitride, and polycrystalline silicon (polysilicon), as commonly done in the literature.[12,14] The absorption coefficients of silicon dioxide and silicon nitride are assumed to be negligible in the wavelength region from 0.5 to 2 μm. The refractive indices are mainly based on the data collected in Refs. 27 and 28 and are assumed to be independent of temperature. A semi-empirical expression for the refractive index of silicon dioxide can be found in Ref. 29 and is used in the present study. The refractive index of silicon dioxide is expressed as

$$n_{\text{SiO}_2} = \left(1 + \frac{0.6961663\lambda^2}{\lambda^2 - 0.0684043^2} + \frac{0.4079426\lambda^2}{\lambda^2 - 0.1162414^2} + \frac{0.8974794\lambda^2}{\lambda^2 - 9.896161^2}\right)^{\frac{1}{2}} \tag{9}$$

In the wavelength range between 0.5 and 1 μm, the refractive index of silicon nitride is assumed as a second-order polynomial of the wavelength and fitted to the data in Ref. 28. The fitted refractive index of silicon nitride is

$$n_{Si_3N_4} = 0.1073\lambda^2 - 0.2420\lambda + 2.133 \tag{10}$$

The optical constants of polysilicon may be different from those of single-crystal silicon because of the presence of the grain boundaries. The main difference between polysilicon and single-crystal silicon is that the absorption edge of polysilicon is broader due to the additional long-wavelength absorption.[30] The refractive index is slightly higher and the extinction coefficient is several times greater than those of single-crystal silicon at wavelengths shorter than the band-gap wavelength, but the differences become smaller at longer wavelengths.[14,31,32] However, the characteristic of polysilicon depends largely on the grain structure resulting from different deposition conditions. In the present study, the optical constants of polysilicon are assumed to be the same as those of single-crystal silicon. The error caused by assuming the optical constants of polysilicon as the same as those of silicon will be further investigated.

Modeling the Radiative Properties of Silicon with Coatings

Because most silicon wafers are thick enough to be opaque in the wavelength range between 0.5 and 1.0 μm, the silicon substrate can be regarded as a semi-infinite medium. Therefore, the wafer with thin-film coatings in the opaque region can be modeled as a multilayer structure of thin films. Consequently, the transfer-matrix method can be used to calculate the radiative properties of a silicon wafer with thin films in the opaque region.[9] In the semitransparent region, interferences in the silicon substrate are generally not observable because the wafer thickness is much greater than the coherence length. The incoherent formulation or geometric optics should be used to predict the radiative properties of the substrate. Two ways to get around this problem are to use the fringe-averaged radiative properties and to treat thin-film coatings as coherent but the substrate as incoherent.[10]

Figure 2 shows the geometry of the silicon wafer with thin-film coatings on both sides. Note that ρ_{ta} and τ_t are the reflectance and transmittance, respectively, of the multilayer structure at the top surface (air–coatings–silicon) for rays incident from air, assuming that the silicon extends to infinite. On the other hand, ρ_{ts} and τ_t are for rays incident from silicon. Note that the transmittance τ_t is the same when absorption inside silicon is negligibly small.[33] Similarly, ρ_{bs} and τ_b are for the multilayer structure at the bottom surface for rays incident from the substrate. In present work, the optical property of air is assumed to be the same as that of vacuum. The transfer-matrix method can be separately applied to calculate the reflectance and transmittance at the top and bottom surfaces of the wafer by neglecting the absorption of silicon. The absorption of silicon can be taken into consideration by introducing the internal transmittance $\tau_i = \exp(-4\pi k_s d_s/\lambda \cos\theta_s)$. Here, k_s is the extinction coefficient of silicon, d_s is the thickness, and θ_s is the angle of refraction. The angle of refraction is complex due to absorption. For a slightly absorbing medium with $k_s \ll 1$, however, θ_s can be determined using Snell's law by neglecting absorption (see Ref. 34). Consequently, the radiative properties of the silicon wafer with thin-film coatings in the semitransparent region can be expressed as[14]

$$\rho = \rho_{ta} + \frac{\tau_i^2 \tau_t^2 \rho_{bs}}{1 - \tau_i^2 \rho_{ts} \rho_{bs}} \tag{11a}$$

$$\tau = \frac{\tau_i \tau_t \tau_b}{1 - \tau_i^2 \rho_{ts} \rho_{bs}} \tag{11b}$$

$$\varepsilon = 1 - \rho - \tau \tag{11c}$$

Because silicon is essentially opaque in the wavelength region from 0.5 to 1.0 μm and the extinction coefficient is several orders smaller than the refractive index ($k \ll n$), small discrepancies in the absorption coefficient can be neglected in calculating the reflectance or emittance. As an extreme case, if we set the extinction coefficient of silicon to be zero at 0.5 μm and room temperature, the calculated reflectance of a bare silicon wafer at normal incidence differs by only 1.16×10^{-4} from the calculated value using $k = 0.073$ from Ref. 15. In the present study, the absorption coefficient of silicon is determined from the J–M expression at $\lambda < 0.9$ μm and the Timans expression at $\lambda \geq 0.9$ μm.

When the refractive index of silicon is calculated, the J–M expression is used in the wavelength region from 0.5 to 0.84 μm, and the Li expression is used at wavelength above 1.2 μm. In the wavelength range between 0.84 and 1.2 μm, we propose a weighted average based on the extrapolation of the two expressions

$$n_{avg} = \frac{(1.2 - \lambda) n_{J\text{–}M} + (\lambda - 0.84) n_L}{1.2 - 0.84} \tag{12}$$

where $n_{J\text{–}M}$ is the refractive index extrapolated from the J–M expression, n_L is from the Li expression, and, again, λ is in micrometers. When the weighted average of the extrapolated expressions is taken as given in Eq. (12), the predicted radiative properties of silicon will be continuous between 0.5 and 5 μm. Therefore, the discontinuity in the predicted radiative properties that is observed in the Multi-RAD can be removed.[12] Notice that beyond 6 μm or so, lattice vibration causes additional absorption and can also affect the refractive index of silicon.

Calculated Results

Figure 3 shows the calculated reflectance for semi-infinite silicon (opaque) with or without coatings, at normal incidence. Because the

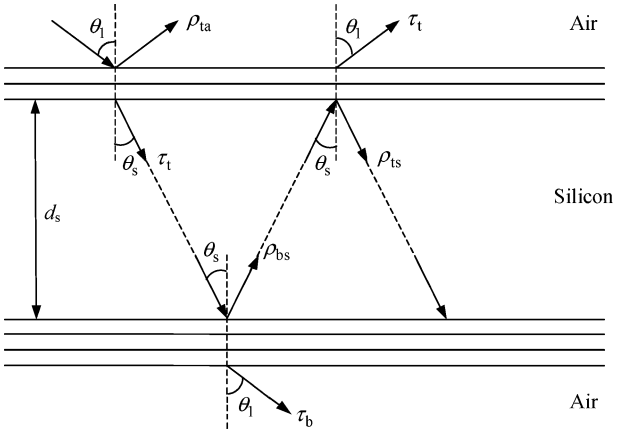

Fig. 2 Schematic of thin-film coatings on both sides of thick silicon substrate.

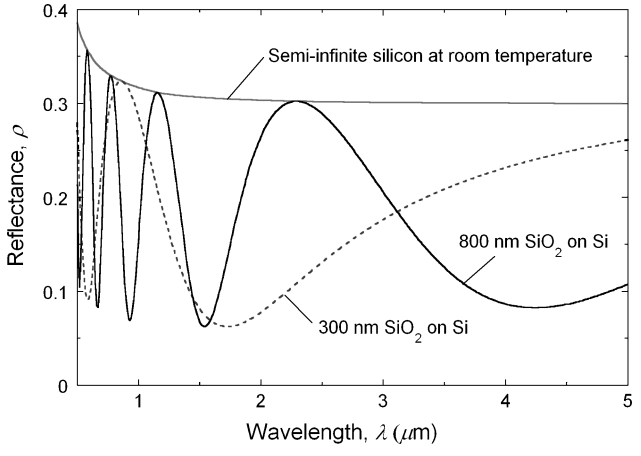

Fig. 3 Room-temperature reflectance of bare silicon and silicon substrate with silicon dioxide coating of 300 nm and 800 nm, respectively; substrate assumed to be semi-infinite.

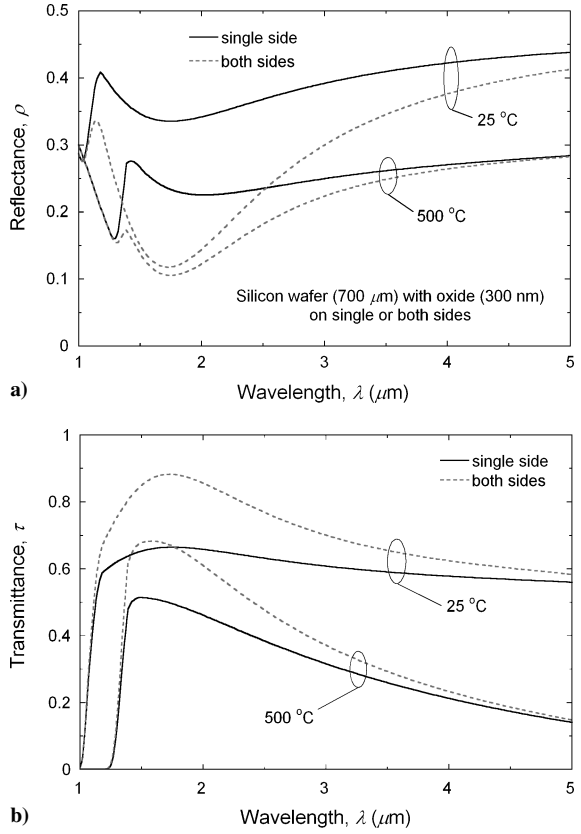

Fig. 4 Silicon wafer, 0.7 mm thick, coated with 300-nm silicon dioxide layer on single side and both sides: a) reflectance and b) transmittance.

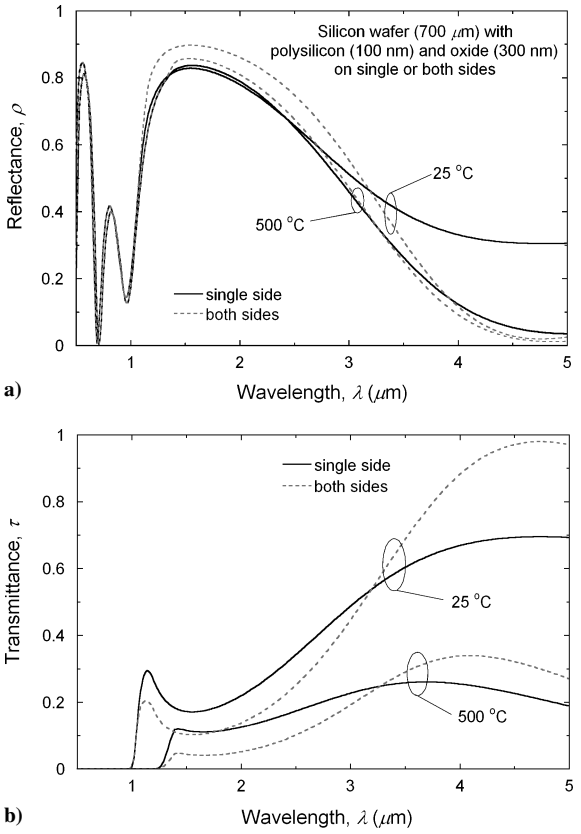

Fig. 5 Silicon wafer, 0.7 mm thick, with oxide and polysilicon layers: a) reflectance and b) transmittance.

refractive index of silicon dioxide (around 1.45) is smaller than that of silicon, the reflectance with a coating is always lower than that of bare silicon. The oscillation in the reflectance is due to interference in the silicon dioxide coating. The free spectral range is determined by $\Delta\lambda/\lambda^2 = (2n_f d_f)^{-1}$, where $\Delta\lambda$ is the separation between adjacent interference maxima and n_f and d_f are the refractive index and thickness of the thin film. The spectral separation $\Delta\lambda$ increases toward longer wavelengths. As the film thickness increases, the free spectral range decreases, resulting in more oscillations with the 800-nm silicon dioxide film.

Figure 4 shows the reflectance and transmittance of a 0.7-mm thick silicon substrate, with single-side and both-side coating of a 300-nm silicon dioxide film, at 25 and 500°C. Although the computation code can deal with different incidence angles and polarizations, only the results for normal incidence are presented here. At $\lambda < 1$ μm, the transmittance is essentially zero, and the reflectance features are similar to those shown in Fig. 3. Hence, the spectra were shown only in the wavelength region between 1 and 5 μm. The increase in temperature causes both the reflectance and transmittance to decrease due to the increase in the absorption coefficient. Therefore, the emittance (not shown in Fig. 4) at 500°C is greater than that at room temperature. The interference effect is enhanced with double-side coatings. The result is an increase in the transmittance and a reduction in the reflectance at certain wavelengths. The emittance changes slightly between the case of single-side and double-side coating.

When a polysilicon (whose optical constants are similar to those of silicon) and an oxide layer are coated on a silicon substrate, very rich features can be seen in the reflectance and transmittance spectra, as shown in Fig. 5. Here, the reflectance can vary from almost zero to one. Again, the increased absorption at elevated temperatures reduces both the reflectance and transmittance. As in the case of Fig. 4, double-side coatings increase the interference effect and result in more changes in the transmittance and reflectance, especially at 25°C when the absorption inside the silicon substrate is relatively small. Because of the interference, the emittance approaches one at $\lambda \approx 0.69$ μm. Because of the high reflectance at around 2 μm, the emittance is very small and depends weakly on the temperature.

Comparison with Reflectance Measurements at Room Temperature

To validate the extrapolation of the existing expressions for the refractive index of silicon, comparison with experimental results is necessary, and room-temperature measurements were performed first in the wavelength range between 0.5 and 1.0 μm. Specular, spectral reflectance of silicon wafers with various thin-film coatings was measured at the National Institute of Standards and Technology using the Cary 5E spectrophotometer, with an integrating sphere, and the spectral trifunction automated reference reflectometer (STARR) for reference measurements. Two specular reference samples were characterized by the STARR, namely, a silicon wafer with a reflectance between 0.3 and 0.4, for relatively low reflectance measurements, and a gold mirror with a reflectance from 0.5 to 0.98, for relatively high reflectance measurements. All measurements were performed with unpolarized light and at an incidence angle of 3.3 deg, which can be considered normal incidence. Even though the geometry of measurement with the Cary 5E spectrophotometer was directional–hemispherical, the specular reflectance of the samples was determined because both they and the reference samples were specular reflectors, and the reference samples were characterized for specular reflectance. The room temperature of the laboratory was between 23 and 25°C. The expanded uncertainty (95% confidence) of the measurement with Cary 5E is 0.003. More detailed descriptions about the instruments can be found in Ref. 35.

Five samples were prepared and studied here. Three are based on single-side-polished p-type ⟨100⟩ silicon with a resistivity of 10 to 50 $\Omega \cdot$cm. One of them is bare silicon, and the other two are coated with a thermal oxide layer (310 nm thick and 850 nm thick, as specified by the supplier). The thickness of the silicon wafer is 0.7 mm. Only the reflectance of the smooth side is measured, and the wafer is essentially opaque for $0.5 \leq \lambda \leq 1$ μm. The other two

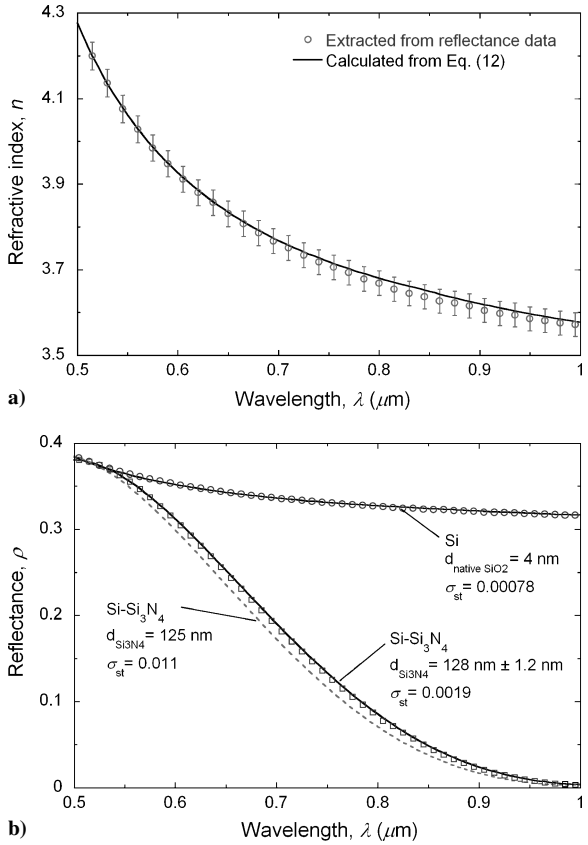

Fig. 6 Refractive index of silicon and reflectance of bare silicon and nitride coated silicon: a) ——, calculated and ○, extracted refractive index and b) ○ and □, measured and ——, fitted reflectance; - - - -, reflectance calculated using thickness provided by supplier.

samples are from double-side-polished p-type ⟨100⟩ silicon with a resistivity of 10 to 25 Ω · cm and a thickness of 0.7 mm. One of the wafers has a silicon nitride coating of 125-nm nominal thickness, and the other has a 170-nm silicon dioxide and 50-nm polysilicon as the top layer. Thin-film coatings are formed on one side only, and the reflectance of the coated side was measured.

Because reflectance is a sensitive function of the coating thickness, a curve fitting was conducted to find the thickness of the coating d_f that minimizes the standard error of estimate between the measured and calculated reflectance,

$$\sigma_{st} = \sqrt{\frac{\sum_{i=1}^{N}[\rho_m(\lambda_i) - \rho_c(\lambda_i; d_f)]^2}{N-1}} \tag{13}$$

where ρ_m and ρ_c are the measured and calculated reflectance, respectively, and N is the total number of data points. The uncertainty of the fitted thickness is estimated by varying d_f from the best-fitted value until σ_{st} is 0.003 greater than the smallest σ_{st}.

Figure 6a shows the refractive index of silicon. The circles represent the refractive index data extracted from the reflectance measurement, and the solid line is that calculated from the functional expression. As mentioned earlier, the effect of k on the reflectance in the wavelengths considered here is negligible compared to the measurement uncertainty. Therefore, when extracting the refractive index from the reflectance measurement, k can be neglected. Consequently, the refractive index of silicon can be extracted from the reflectance measurement using $1 - \rho = 4n_s/(n_s + 1)^2$, where n_s refers to the refractive index of the silicon wafer, for near normal incidence.[16] It is clear that the calculated refractive index values agree well with those extracted from the measurement, and 0.6% variations of n from the functional expression cause the change in the reflectance by the measurement uncertainty. Therefore, it can be inferred that the functional expression for the refractive index of silicon is good, with 0.6% relative errors.

The reflectance of the bare silicon wafer and the sample with a silicon nitride coating is shown in Fig. 6b. The circles and squares are the measured data, and solid lines are the calculated reflectance, based on the assumed expressions of the optical constants of silicon and the refractive index value of silicon nitride. Because it is believed that a native oxide layer of 2–4 nm exists on top of the bare silicon wafer, the reflectance of bare silicon is fitted by assuming a thin silicon dioxide layer to improve the fitting result. The best-fitted value of the thickness is 4 nm with $\sigma_{st} = 0.00078$. However, if the native oxide layer thickness is assumed to be zero, then the calculated σ_{st} is 0.00095. If the oxide layer thickness is taken as 8 nm, the corresponding σ_{st} is 0.0019, which is still within the measurement uncertainty. Therefore, the native oxide has little effect on the reflectance.

When the silicon substrate is coated with an SiO_2 or Si_3N_4 film, which serves as an antireflection coating, the reflectance oscillates from a minimum to a maximum, equal to the reflectance of silicon without coating. The reflectance minimum is independent of the coating thickness and is given by $\rho_{\min} = [(n_a n_s - n_f^2)/(n_a n_s + n_f^2)]^2$, where $n_a = 1$ is the refractive index of air.[36] As shown in Fig. 6b, the reflectance minimum for nitride-coated wafer is 0.0029 at $\lambda = 1$ μm. The refractive index of Si_3N_4 extracted from the reflectance minimum is 1.995, which is almost the same as the value of 1.998 calculated from Eq. (10). When the reflectance is very low, the absolute uncertainty of 0.003 is not appropriate; therefore, a relative uncertainty of 30% is assumed for the measured minimum reflectance of the nitride-coated wafer. Together with the uncertainty of 0.6% in the refractive index of silicon, the uncertainty of the refractive index of Si_3N_4 calculated from Eq. (10) is estimated to be 1%. The spectral reflectance is a strong function of the film thickness, and the measured spectrum can be fitted by taking the thickness as an adjustable parameter using the expressions of the optical constants of silicon and nitride. The best-fitted nitride thickness is 128 nm ± 1.2 nm with $\sigma_{st} = 0.0019$. Figure 6b also shows the reflectance calculated using the Si_3N_4 thickness of 125 nm, provided by the supplier. Note that there is a significant disagreement and the calculated σ_{st} is 0.011. Because σ_{st} of the curve fitting is very sensitive to the variation of the coating thickness, the thickness obtained by the present work has a much smaller uncertainty due to the high accuracy in the reflectance measurement. Zhang et al.[37] obtained both the refractive index and film thickness of a free-standing film by fitting the transmittance spectra, and they discussed the advantage of using the spectrometric method in determination of the film thickness.

The reflectance of wafers with thermal oxide coatings is shown in Fig. 7, together with the calculated values for silicon. Interference effects in the silicon dioxide films can be clearly seen. The

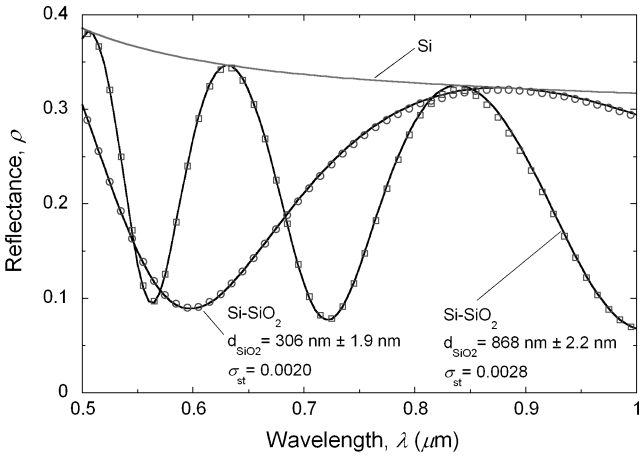

Fig. 7 Comparison of ○ and □, measured and ——, calculated reflectance for silicon wafers with thermal oxide coating of two different thicknesses; calculated reflectance curve of bare silicon is plotted for comparison purpose, and best-fitted coating thickness with uncertainty and standard error of estimate are indicated.

Table 1 Results of reflectance curve fitting for the five samples

Sample	Bare silicon	Si–Si_3N_4	Si–SiO_2	Si–SiO_2	Si–SiO_2–polysilicon
Coating thickness,[a] nm	2 to 4 (native oxide)	125	310	850	(SiO_2/polysilicon) 170/50
σ_{st}	0.00095	0.011	0.0092	0.043	0.044
Coating thickness,[b] nm	4	128	306	868	163/55
σ_{st}[b]	0.00078	0.0019	0.0020	0.0028	0.0053
Relative difference, %	——	2.3	1.3	2.0	4.3/9.0
Uncertainty of fitted thickness, nm	——	±1.2	±1.9	±2.2	±1.2/±0.5

[a]Value from supplier. [b]Best-fitted value.

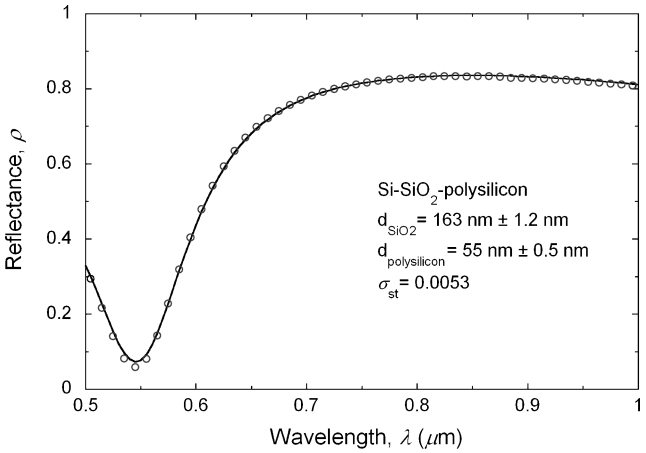

Fig. 8 Comparison of ○, measured and ——, calculated reflectance of silicon wafer with polysilicon layer over a thermal oxide layer; best-fitted coating thickness with uncertainty and standard error of estimate are indicated.

spectral separation between interference peaks decreases as the film thickness increases. As a consequence, there are more oscillations for the sample with a thicker oxide layer. Because SiO_2 also serves as an antireflection coating, from the reflectance minimum, n_{SiO_2} is determined to be 1.452 at $\lambda = 0.565\ \mu$m, 1.455 at $\lambda = 0.6\ \mu$m, and 1.452 at $\lambda = 0.72\ \mu$m. When refractive index values determined from reflectance minimum are compared to those calculated from Eq. (9), the uncertainty of this expression is estimated to be within 1%. Similar to the nitride-coated sample, the reflectance for the oxide-coated samples is fitted by varying the coating thickness. For the sample with a thin oxide layer, the fitted thickness is 306 nm ± 1.9 nm with $\sigma_{st} = 0.0020$, and differs by only 4 nm, or 1.3%, from the value provided by the supplier. For the sample with a thick oxide layer, the fitted thickness is 868 nm ± 2.2 nm with $\sigma_{st} = 0.0028$, and differs by 18 nm, or 2%, from the value provided by the supplier.

Table 1 summarizes the result of the reflectance curve fitting for all studied samples. The standard error of estimate between the measured and calculated reflectance when the thin-film coating thickness is equal to the value provided by the supplier is almost an order of magnitude higher than that for the best-fitted value. The excellent agreement of the fitted with the measured reflectance of oxide indicates that the thicknesses obtained in the present study are more accurate and reliable than those specified by the supplier. The estimated uncertainty of the fitted thickness is less than 1% for all cases. In addition, σ_{st} of the best fitting is within the measurement uncertainty, except for the sample with two coating layers, as discussed hereafter.

Figure 8 shows the reflectance of the silicon wafer with a 50-nm polysilicon film on top of a 170-nm silicon dioxide coating. Wave interferences inside the two layers have caused a reflectance that is more than twice as high as that of bare silicon at certain wavelengths, but much lower at some other wavelengths. Because the reflectance is high at longer wavelengths, the gold reference is used in the measurement. When more than one film is coated on the wafer, the reflectance minimum depends strongly on the wavelength, as well as on the refractive index and thickness of each film. One cannot use the reflectance minimum to determine the refractive index independently of the film thickness. Therefore, the measured reflectance spectrum is fitted by varying two coating thicknesses, assuming that the refractive index of polysilicon is the same as that of silicon. The best-fitted thickness values are obtained by trial-and-error to minimize σ_{st} between the calculated and measured reflectance. The fitted silicon dioxide thickness is 163 nm ± 1.2 nm, and the polysilicon thickness is 55 nm ± 0.5 nm. These values are within 7 nm (4.3%) and 5 nm (9%) of those provided by the supplier, respectively. The σ_{st} is 0.0053, which is nearly twice the expanded uncertainty of the reflectance measurement. The large σ_{st} may be caused by assuming that the optical constants of the polysilicon are the same as those of single-crystal silicon. Further study is needed to determine accurately the optical constants of the polysilicon film.

Conclusions

The present paper describes several carefully selected model expressions for calculating the optical constants of lightly doped silicon. Extrapolations were made to produce smooth curves in the calculated radiative properties. A hybrid model based on thin-film optics (for coatings on one or both sides of the wafers) and incoherent formulation (for rays inside the thick silicon substrate) was employed to study the effects of coating thickness, types of coating, and temperature on the radiative properties of silicon wafers.

An experimental validation was performed on the model expressions for the refractive index of silicon and related materials at room temperature. The reflectance was measured over the wavelength region from 0.5 to 1.0 μm for five samples and compared with the calculated values using thin-film optics. The excellent agreement between the measured and calculated reflectance suggests that the extrapolation of the expressions for the refractive index of silicon to the wavelength region between 0.84 and 1.0 μm is appropriate at room temperature. The excellent agreement in the reflectance minimum confirms the expressions for the optical constants of silicon dioxide and silicon nitride. The calculated reflectance spectrum was fitted to the measured values by changing the thickness of the thin-film coatings. This allows accurate determination of the coating thickness for single-layer coatings. However, a larger deviation exists for a silicon wafer coated with polysilicon and silicon oxide films, suggesting that further study of the optical constants of polysilicon is needed.

This study serves as an initial step toward a better understanding of the radiative properties of silicon-related materials for accurate radiometric temperature measurements in RTP systems. It is imperative to validate the expressions of optical constants at the processing conditions. The same samples could be used in the future because the coating thicknesses have been accurately determined through the present work.

Acknowledgments

This work was made possible by the financial support from the National Institute of Standards and Technology Office of Microelectronics Program and the National Science Foundation (CTS-0236831).

References

[1]Roozeboom, F., and Parekh, N., "Rapid Thermal Processing Systems: A Review with Emphasis on Temperature Control," *Journal of Vacuum Science and Technology B*, Vol. 8, No. 6, 1990, pp. 1249–1259.

[2]Timans, P. J., "Rapid Thermal Processing Technology for the 21st Century," *Materials Science in Semiconductor Processing*, Vol. 1, Nos. 3–4, 1998, pp. 169–179.

[3]Zhang, Z. M., "Surface Temperature Measurement Using Optical Techniques," *Annual Review of Heat Transfer*, edited by C. L. Tien, Vol. 11, Begell House, New York, 2000, pp. 351–411.

[4]Zhou, Y. H., Shen, Y. J., Zhang, Z. M., Tsai, B. K., and DeWitt, D. P., "A Monte Carlo Model for Predicting the Effective Emissivity of the Silicon Wafer in Rapid Thermal Processing Furnaces," *International Journal of Heat and Mass Transfer*, Vol. 45, No. 9, 2002, pp. 1945–1949.

[5]Adams, B., Hunter, A., Yam, M., and Peuse, B., "Determining the Uncertainty of Wafer Temperature Measurements Induced by Variations in the Optical Properties of Common Semiconductor Materials," *Rapid Thermal and Other Short-Time Processing Technologies: Proceedings of the International Symposium*, Vol. 2000-9, Electrochemical Society, Pennington, NJ, 2000, pp. 363–374.

[6]Shen, Y. J., Zhang, Z. M., Tsai, B. K., and DeWitt, D. P., "Bidirectional Reflectance Distribution Function of Rough Silicon Wafers," *International Journal of Thermophysics*, Vol. 22, No. 4, 2001, pp. 1311–1326.

[7]Tang, K., and Buckius, R. O., "A Statistical Model of Wave Scattering from Random Rough Surfaces," *International Journal of Heat and Mass Transfer*, Vol. 44, No. 21, 2001, pp. 4059–4073.

[8]Zhou, Y. H., and Zhang, Z. M., "Radiative Properties of Semitransparent Silicon Wafers with Rough Surfaces," *Journal of Heat Transfer,* Vol. 125, No. 3, 2003, pp. 462–470.

[9]Yeh, P., *Optical Waves in Layered Media,* Wiley, New York, 1998, Chap. 5.

[10]Zhang, Z. M., Fu, C. J., and Zhu, Q. Z., "Optical and Thermal Radiative Properties of Semiconductors Related to Micro/Nanotechnology," *Advances in Heat Transfer*, Vol. 37, 2003, pp. 179–296.

[11]Cohen, M. L., and Chelikowsky, J. R., *Electronic Structure and Optical Properties of Semiconductors*, 2nd edition, Springer-Verlag, Berlin, 1988, Chap. 8.

[12]Hebb, J. P., "Pattern Effects in Rapid Thermal Processing," Ph.D. Dissertation, Dept. of Mechanical Engineering, Massachusetts Inst. of Technology, Cambridge, MA, 1997.

[13]Ravindra, N. M., Sopori, B., Gokce, O. H., Cheng, S. X., Shenoy, A., Jin, L., Abedrabbo, S., Chen, W., and Zhang, Y., "Emissivity Measurements and Modeling of Silicon-Related Materials: An Overview," *International Journal of Thermophysics*, Vol. 22, No. 5, 2001, pp. 1593–1611.

[14]Timans, P. J., "The Thermal Radiative Properties of Semiconductors," *Advances in Rapid Thermal and Integrated Processing*, edited by F. Roozeboom, Kluwer Academic, Dordrecht, The Netherlands, 1996, Chap. 2.

[15]Edwards, D. F., "Silicon (Si)," *Handbook of Optical Constants of Solids*, edited by E. D. Palik, Academic Press, Orlando, 1985, pp. 547–569.

[16]Sato, T., "Spectral Emissivity of Silicon," *Japanese Journal of Applied Physics*, Vol. 6, No. 3, 1967, pp. 339–347.

[17]Jellison, G. E., Jr., and Modine, F. A., "Optical Functions of Silicon at Elevated Temperatures," *Journal of Applied Physics*, Vol. 76, No. 6, 1994, pp. 3758–3761.

[18]Li, H. H., "Refractive Index of Silicon and Germanium and Its Wavelength and Temperature Derivatives," *Journal of Physical and Chemical Reference Data,* Vol. 9, No. 3, 1980, pp. 561–658.

[19]Magunov, A. N., "Temperature Dependence of the Refractive Index of Silicon Single Crystal in the 300–700 K Range," *Optics and Spectroscopy*, Vol. 73, No. 2, 1992, pp. 205, 206.

[20]Magunov, A. N., and Mudrov, E. V., "Optical Properties of Lightly Doped Single-Crystal Silicon Near the Absorption Edge at 300–700 K," *Optics and Spectroscopy,* Vol. 70, No. 1, 1991, pp. 83–85.

[21]Timans, P. J., "Emissivity of Silicon at Elevated Temperature," *Journal of Applied Physics,* Vol. 74, No. 10, 1993, pp. 6353–6364.

[22]MacFarlane, G. G., McLean, T. P., Quarrington, J. E., and Roberts, V., "Fine Structure in the Absorption-Edge Spectrum of Si," *Physical Review,* Vol. 111, No. 5, 1958, pp. 1245–1254.

[23]Sturm, J. C., and Reaves, C. M., "Silicon Temperature Measurement by Infrared Absorption: Fundamental Processes and Doping Effects," *IEEE Transactions on Electron Devices*, Vol. 39, No. 1, 1992, pp. 81–88.

[24]Vandenabeele, P., and Maex, K., "Influence of Temperature and Backside Roughness on the Emissivity of Si Wafers During Rapid Thermal Processing," *Journal of Applied Physics,* Vol. 72, No. 12, 1992, pp. 5867–5875.

[25]Rogne, H., Timans, P. J., and Ahmed, H., "Infrared Absorption in Silicon at Elevated Temperatures," *Applied Physics Letters,* Vol. 69, No. 15, 1996, pp. 2190–2192.

[26]Saritas, M., and McKell, H. D., "Absorption Coefficient of Si in the Wavelength Region Between 0.80–1.16 μm," *Journal of Applied Physics*, Vol. 61, No. 10, 1987, pp. 4923–4925.

[27]Philipp, H. R., "Silicon Dioxide (SiO_2) (Glass)," *Handbook of Optical Constants of Solids*, edited by E. D. Palik, Academic Press, Orlando, 1985, pp. 749–763.

[28]Philipp, H. R., "Silicon Nitride (Si_3N_4) (Noncrystalline)," *Handbook of Optical Constants of Solids*, edited by E. D. Palik, Academic Press, Orlando, 1985, pp. 771–774.

[29]Maltison, I. H., "Interspecimen Comparison of the Refractive Index of Fused Silica," *Journal of the Optical Society of America,* Vol. 55, No. 10, 1965, pp. 1205–1209.

[30]Clark, A. H., "Optical Properties of Polycrystalline Semiconductor Films," *Polycrystalline and Amorphous Thin Films and Devices*, edited by L. L. Kazmerski, Academic Press, New York, 1980, pp. 135–152.

[31]Jellison, G. E., Jr., Keefer, M., and Thornquist, L., "Spectroscopic Ellipsometry and Interference Reflectometry Measurements of CVD Silicon Grown on Oxidized Silicon," *Proceedings of the Materials Research Society Symposium*, Vol. 283, Materials Research Society, Pittsburgh, PA, 1993, pp. 561–566.

[32]Lubberts, G., Burkey, B. C., Moser, F., and Trabka, E. A., "Optical Properties of Phosphorus-Doped Polycrystalline Silicon Layers," *Journal of Applied Physics*, Vol. 52, No. 11, 1981, pp. 6870–6878.

[33]Zhang, Z. M., "Reexamination of the Transmittance Formulae of a Lamina," *Journal of Heat Transfer*, Vol. 119, No. 3, 1997, pp. 645–647.

[34]Zhang, Z. M., "Optical Properties of a Slightly Absorbing Film for Oblique Incidence," *Applied Optics*, Vol. 38, No. 1, 1999, pp. 205–207.

[35]Barnes, P. Y., Early, E. A., and Parr, A. C., *Spectral Reflectance*, Special Publ. 250-48, National Inst. of Standards and Technology, Gaithersburg, MD, 1998, pp. 40–48.

[36]Born, M., and Wolf, E., *Principles of Optics*, Cambridge Univ. Press, Cambridge, England, U.K., 2002, Chap. 1.

[37]Zhang, Z. M., Lefever-Button, G., and Rowell, F. R., "Infrared Refractive Index and Extinction Coefficient of Polyimide Films," *International Journal of Thermophysics*, Vol. 19, No. 3, 1998, pp. 905–916.